Journal of Chromatography, 517 (1990) 345–359
Elsevier Science Publishers B.V., Amsterdam

CHROMSYMP. 1944

Potential-barrier field-flow fractionation, a versatile new separation method

A. KOLIADIMA and G. KARAISKAKIS*
Department of Chemistry, University of Patras, GR-26110 Patras (Greece)

ABSTRACT

A new method called potential-barrier field-flow fractionation, which is a combination of potential-barrier chromatography and sedimentation field-flow fractionation (SdFFF), is presented for the separation and characterization of colloidal materials. The separation is based either on particle size differences or on Hamaker constant, surface potential and Debye–Hückel reciprocal distance differences. In its simplest form the technique consists in changing the ionic strength of the carrier solution from a high value, where only one of the colloidal materials of the binary mixture subjected to separation is totally adsorbed at the beginning of the SdFFF channel wall, to a lower value, where the total number of adhered particles is released. The method was applied to the separation of haematite and titanium dioxide spherical colloidal particles and to the separation of haematite spherical particles with different sizes. At the same time as separation was occurring, the particle sizes of the colloidal materials of the mixture were determined. The experimental values of particle diameters were in good agreement with those obtained by transmission electron microscopy or determined by normal SdFFF. Finally, the retention perturbations due to particle (α-Fe_2O_3 and TiO_2)–wall interactions in SdFFF were investigated.

INTRODUCTION

During the last few years, interest has arisen in methods for the separation of suspended particles, in analogy with techniques used for matter in solution. Hydrodynamic chromatography[1], gel chromatography[2], potential-barrier chromatography[3] and field-flow fractionation (FFF)[4–8] have already been studied, and potential-barrier FFF (PBFFF) has recently been suggested[9,10]. The latter is a combination of FFF and potential-barrier chromatography.

Basically, FFF is a one phase-chromatographic system in which an external field or gradient replaces the stationary phase. The applied field can be of any type that interacts with the sample components and causes them to move perpendicular to the flow direction in the open channel. The most highly developed of the various FFF modes is sedimentation FFF (SdFFF), in which the separations of suspended parti-

0021-9673/90/$03.50

cles are performed with a single, continuously flowing mobile phase in a very thin, open channel under the influence of an external centrifugal force field[4].

SdFFF yields experimental data in the form of a fractogram, which is a plot of the detector response of the emerging sample *versus* the time or volume of its emergence. For constant field conditions, the retention volume (or time) in SdFFF is immediately related to the particle mass. Thus, in normal SdFFF, where the particle–wall interactions are negligible, the separation is based on particle size differences.

Potential-barrier chromatography (PBC) can be applied to separate particles based on differences in size or in any of the physico-chemical parameters involved in the potential energy of interaction between the particles and the packing of the column. This method, which is based on the existence of a surmountable potential barrier between particles and deposition surface, is classified as an FFF method rather than a chromatographic method, because the selective interaction is experienced in one phase. Thus, by combining PBC with normal SdFFF one could separate according to two mechanisms, one governed by the depth of the potential energy well for the different particles and the other determined by the interactive force between the particles and the external field.

The purpose of this work was to study the interactions between the particle and the channel wall in SdFFF and to show the applicability of PBFFF in the separation of colloidal particles.

THEORY

In normal SdFFF, where the particle–wall interactions are absent, the potential energy of a spherical particle is given by the relation[10]

$$V(x) = \frac{\pi d^3}{6}(\rho_s - \rho)Gx = \frac{\pi d^3}{6} \cdot \Delta\rho Gx \tag{1}$$

where d is the diameter and ρ_s the density of the spherical particle, ρ is the carrier density, G is the sedimentation field strength expressed as acceleration and x is the coordinate position of the centre of particle mass.

The retention ratio, R, in SdFFF is given by the ratio of the column void volume, V_0, to the component retention volume, V_R. For highly retained peaks and spherical particles, R can be expressed as

$$R = \frac{V_0}{V_R} \approx 6\lambda = \frac{6l}{w} = \frac{36kT}{\pi d^3 Gw\Delta\rho} \tag{2}$$

where l is the characteristic mean layer thickness of the solute, w is the channel thickness, λ ($= l/w$) is a dimensionless retention parameter, k is Boltzmann's constant and T is the absolute temperature.

When the colloidal particles interact with the SdFFF channel wall, the potential energy given by eqn. 1 must be corrected by considering the potential energy of

interaction $V(h)$. The latter can be estimated by the sum of the contributions of the Van der Waals, $V_6(h)$, and double-layer, $V_{DL}(h)$, forces:

$$V(h) = V_6(h) + V_{DL}(h) \tag{3}$$

where h is the separation distance between the sphere and the channel wall.

The Van der Waals interaction energy is approximated by[3]

$$V_6(h) = \frac{A_{132}}{6}\left[\ln\left(\frac{h+2\alpha}{h}\right) - \frac{2\alpha(h+\alpha)}{h(h+2\alpha)}\right] \tag{4}$$

where α is the particle radius and A_{132} is the effective Hamaker constant for media 1 and 2 interacting across medium 3. Combining laws are frequently used for obtaining approximate values for unknown Hamaker constants in terms of known values. The constant A_{132} can be approximately related to A_{131} and A_{232} via[11]

$$A_{132} \approx \sqrt{A_{131}A_{232}} \tag{5}$$

where A_{131} represents the interaction of two nearby bodies of material 1, separated by medium 3. A corresponding meaning applies to A_{232}. Two other useful relationships developed by Israelachvili[11] are the following:

$$A_{131} \approx \left(\sqrt{A_{11}} - \sqrt{A_{33}}\right)^2 \tag{6}$$

$$A_{232} \approx \left(\sqrt{A_{22}} - \sqrt{A_{33}}\right)^2 \tag{7}$$

which when combined with eqn. 5 give

$$A_{132} \approx \left(\sqrt{A_{11}} - \sqrt{A_{33}}\right)\left(\sqrt{A_{22}} - \sqrt{A_{33}}\right) \tag{8}$$

The Hamaker constants can be calculated on the basis of the Lifshitz theory from the relationship[11]

$$A_{132} \approx \frac{3h\nu_e}{8\sqrt{2}} \cdot \frac{(n_1^2 - n_3^2)(n_2^2 - n_3^2)}{(n_1^2 + n_3^2)^{\frac{1}{2}}(n_2^2 + n_3^2)^{\frac{1}{2}}[(n_1^2 + n_3^2)^{\frac{1}{2}} + (n_2^2 + n_3^2)^{\frac{1}{2}}]} + \\ + \frac{3}{4}kT\left(\frac{\varepsilon_1 - \varepsilon_3}{\varepsilon_1 + \varepsilon_3}\right)\left(\frac{\varepsilon_2 - \varepsilon_3}{\varepsilon_2 + \varepsilon_3}\right) \tag{9}$$

where n_1, n_2 and n_3 are the refractive indices of the three media, ε_1, ε_2 and ε_3 are the corresponding static dielectric constants and ν_e is the mean value of the absorption frequency of the three media.

The Hamaker constants A_{ii} can also be determined experimentally by measuring the corresponding surface tensions, since[11]

$$A_{ii} \approx 2.1 \cdot 10^{-21} \gamma_{ii} \tag{10}$$

where γ_{ii} is in mJ m^{-2} and A in J.

Eqn. 4 shows that the energy $V_6(h)$ depends on the Hamaker constant and on the particle radius, α.

The double-layer interaction potential, resulting from the development of electrical double layers at the solid–liquid interfaces is given by[3]

$$V_{DL}(h) = 16\varepsilon\alpha\left(\frac{kT}{e}\right)^2 \tanh\left(\frac{e\psi_1}{4kT}\right)\tanh\left(\frac{e\psi_2}{4kT}\right)e^{-\kappa h} \tag{11}$$

where ε is the dielectric constant of the liquid phase, e is the electronic charge, ψ_1 and ψ_2 are the surface potentials of the solid surfaces and κ is the reciprocal Debye length.

For oxides in water, as is the case here, the surface potential, ψ, is determined by the pH of the solution, as H^+ and OH^- are potential-determining ions. The potential is given by[12]

$$\psi = \frac{kT}{2.303e}(pH_{zpc} - pH) \tag{12}$$

where pH_{zpc} is the pH at which the net charge on the surface is zero.

For comparison purposes, apart from the surface potential, one could use the ζ potential calculated from the electrophoretic mobility, u, via the equations[13]

$$\zeta = \frac{6\pi n u}{\varepsilon} \qquad (\kappa\alpha \ll 1) \tag{13}$$

$$\zeta = \frac{4\pi n u}{\varepsilon} \qquad (\kappa\alpha \gg 1) \tag{14}$$

where n is the viscosity and ε is the dielectric constant of the suspending medium.

The reciprocal double-layer thickness is given by the expression

$$\kappa^{-1} = BI^{-\frac{1}{2}} \tag{15}$$

where B is a constant and I is the ionic strength of the suspending medium.

Eqns. 11 and 15 show that the energy $V_{DL}(h)$ is influenced from the surface potentials, ψ_1 and ψ_2, the ionic strength, I, and the particle radius, α.

The total potential energy, V_{tot}, of a spherical particle in PBFFF will equal the sum of the expressions in eqns. 1, 4 and 11:

$$V_{tot} = \frac{4}{3}\pi\alpha^3 \Delta\rho G x + \frac{A_{132}}{6}\left[\ln\left(\frac{h+2\alpha}{h}\right) - \frac{2\alpha(h+\alpha)}{h(h+2\alpha)}\right] + \\ + 16\varepsilon\alpha\left(\frac{kT}{e}\right)^2 \tanh\left(\frac{e\psi_1}{4kT}\right)\tanh\left(\frac{e\psi_2}{4kT}\right)e^{-\kappa h} \quad (16)$$

The last equation shows that the energy V_{tot} in PBFFF (at a given SdFFF system, where the surface potential of the wall ψ_2 is constant) is a function of the size and of the surface potential of the particle, of the Hamaker constant and of the ionic strength of the carrier solution.

EXPERIMENTAL

The experimental procedure has been described in detail elsewhere[6,8,14]. The two SdFFF systems used in this work had the following dimensions: system I, 38.4 × 2.05 × 0.0262 cm^3 with a channel void volume of 2.06 cm^3, measured by the elution of the non-retained peak of sodium benzoate; system II, 38.5 × 2.3 × 0.0181 cm^3 with a channel void volume of 1.60 cm^3. In both systems the column was 6.85 cm from the centre of rotation. A Gilson Holochrome UV detector was used for detection at 254 nm and a Gilson Minipuls 2 peristaltic pump was used to pump the carrier solution and the sample to the channel.

The electrophoretic mobilities of α-Fe_2O_3 and TiO_2 particles were measured in a microelectrophoresis apparatus (Rank, Mark II) by using a four-electrode capillary cell. The velocities of at least twenty particles in each direction of the electric field were measured at the two stationary layers with an accuracy of ± 10%. The pH of the colloidal suspensions was measured by using a combination glass–saturated calomel electrode (Metrohm).

For the identification of the type of modification of TiO_2, a Philips Model PW 1130/00 X-ray diffractometer was used. The form of TiO_2 was found to be anatase. The transmission electron microscopic (TEM) pictures for the α-Fe_2O_3 and TiO_2 particles, some examples of which are shown in Fig. 1, were taken with a JEOL Model JSM-2 transmission electron microscope.

The surface tensions of the titanium dioxide and haematite colloidal particles were measured with a torsion balance from White Electrical Instruments.

Titanium dioxide monodisperse colloidal particles from PolySciences with an average diameter (obtained by TEM) of 0.388 μm, and haematite nearly monodisperse colloidal particles of two sizes (α-Fe_2O_3(I) with d = 0.148 μm and α-Fe_2O_3(II) with d = 0.248 μm, supplied by Prof. J. Lyklema (Agricultural University, Wageningen, The Netherlands) were used as samples.

The carrier was triply distilled water containing 0.5% (v/v) of detergent FL-70 and 0.02% (w/w) sodium azide as bacteriocide. The electrolyte added to this carrier solution in order to adjust its ionic strength was potassium nitrate from Riedel-de Haën. The ionic strength of FL-70 alone was taken to be 10^{-3} M from conductivity measurements.

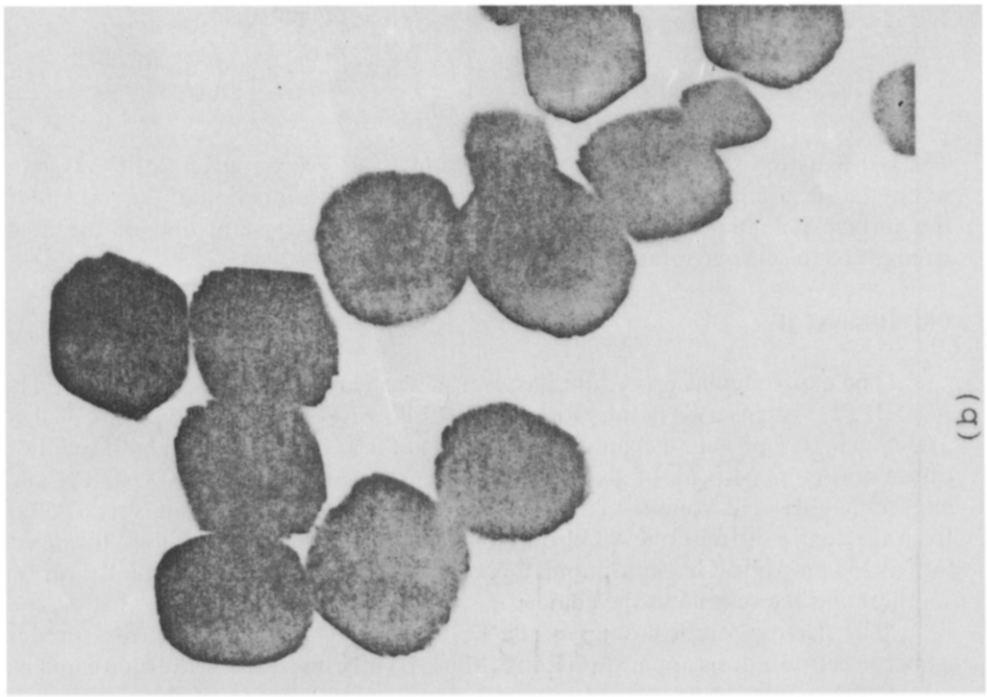
(b)

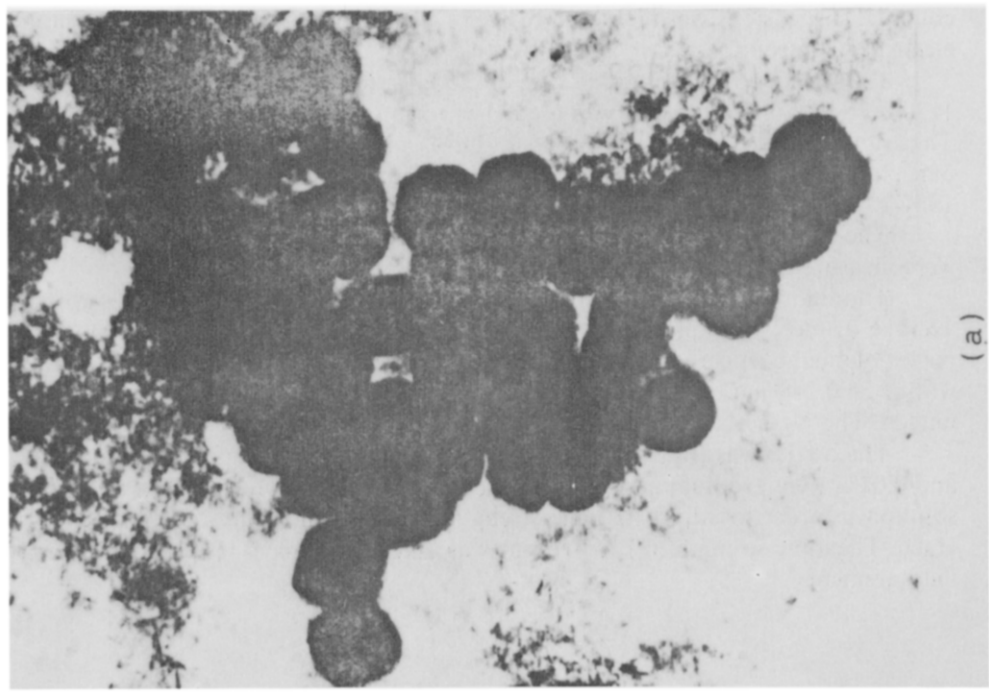
(a)

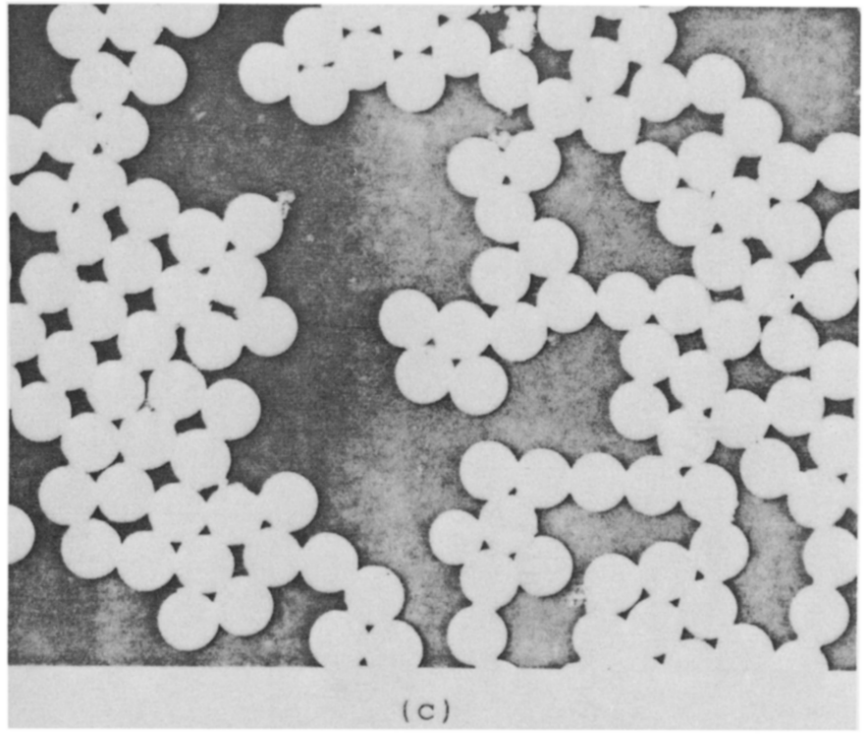

Fig. 1. Transmission electron micrographs: (a) haematite-I (80 000 ×); (b) haematite-II (80 000 ×); (c) TiO_2 (20 000 ×).

RESULTS AND DISCUSSION

Interactions between haematite and the SdFFF channel wall

Haematite-I (H-I, d_{TEM} = 0.148 μm). In order to select the optimum experimental conditions for minimizing the interactions between H-I and the SdFFF channel wall, the retention ratios or the particle diameters of the H-I particles were measured at various field strengths and at a constant flow-rate, and also at various flow-rates and at a constant field strength.

Fig. 2a, in which the variation of the experimental diameter, $d^{exp.}$, with the field strength and the constant theoretical diameter, d^{TEM} (determined by TEM) are presented, shows that the optimum field strength for H-I is $G = 15\,212$ cm s^{-2} (450 rpm). The optimum flowrate found from Fig. 2b, which shows the variation of $d^{exp.}$ with the carrier flow-rate at a constant field strength and constant d^{TEM} value, is *ca.* 150 cm^3 h^{-1}. Ideally, no differences should be observed with varying field and flow conditions. However, with increasing field strength the interaction between the particles and the SdFFF channel wall is intensified. Further, the increase in flow-rate offsets the interaction, as the hydrodynamic lift forces accelerate elution. Of course, more experimental work is necessary in order to investigate these variations.

Using the optimum experimental conditions found ($G = 15\,212$ cm s^{-2}, $\dot{V} =$ 150 cm^3 h^{-1}) the variation of the retention ratio or of the particle diameter with the ionic strength of the carrier solution was investigated. Fig. 3 illustrates the results of a series of retention measurements at different ionic strengths for the heamatite sample H-I with a nominal diameter of 0.148 μm in the stainless-steel channel wall and with two carrier flow-rates. At both carrier flow-rates for the more concentrated solutions (*ca.* $3 \cdot 10^{-2}$ *M* KNO_3), the retention ratio decreased and the particle diameter was higher than the theoretical value, although the data points in Fig. 3a have a relatively large random error.

The above observations are in accord with the analysis of particle–wall interactions presented under Theory. It was predicted there that at higher ionic strengths the

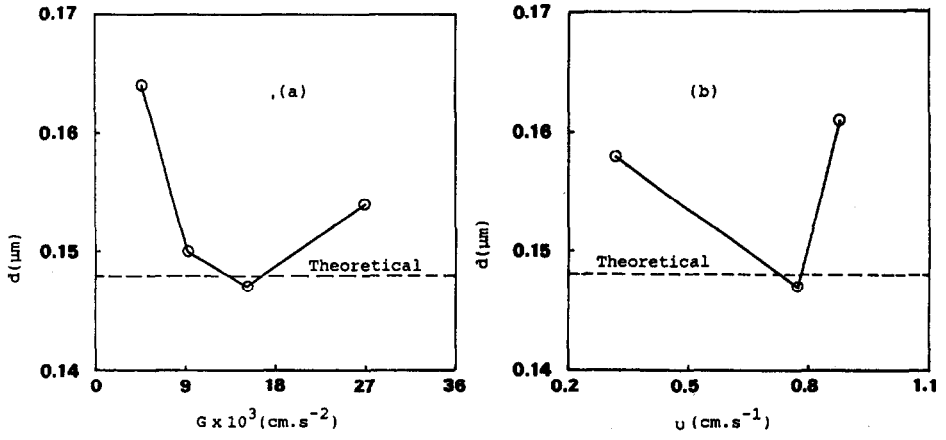

Fig. 2. Variation of particle diameter for the haematite-I sample (a) with the field strength at a constant flow-rate and (b) with the carrier flow-rate at a constant field strength. In both instances the SdFFF system I was used.

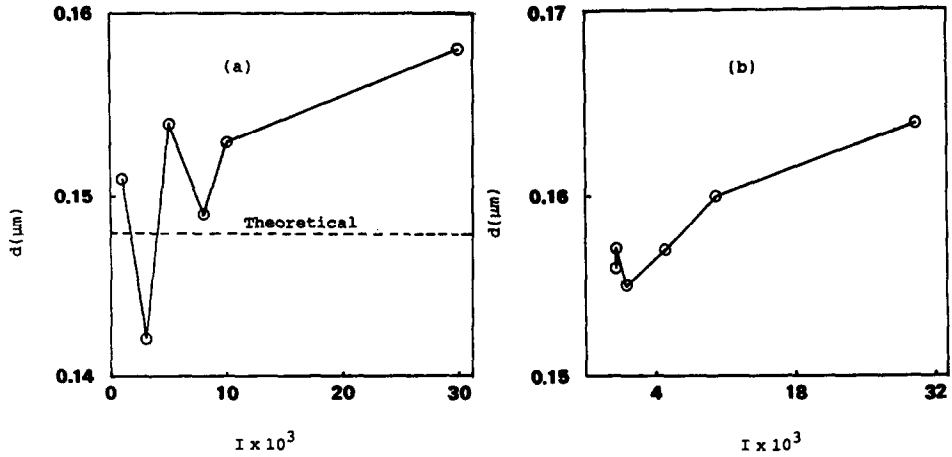

Fig. 3. Variation of the particle diameter for the haematite-I sample with the ionic strength of the carrier solution at 450 rpm. Flow-rate: (a) 150 and (b) 60 $cm^3\ h^{-1}$. In both instances the SdFFF system I was used.

attractive forces play an increasing role, eventually leading to a decrease in the R value and subsequently to an increase in the d value. Changing the carrier solution to one containing a higher concentration of KNO_3 (*ca.* $5 \cdot 10^{-2}$ M) led to the adsorption of all of the H-I particles on the stainless-steel channel wall, as no elution curve was obtained. In the system under investigation, in which the α-Fe_2O_3 particles and the collector (stainless-steel channel wall) carry charges of the same sign (both are negative), the deposition of the particles on the SdFFF channell wall at high electrolyte concentrations is due to the compression of the double layer. When the carrier solution was changed to one containing a lower ionic strength (*ca.* 10^{-3} M KNO_3), a sample peak appeared as a consequence of the desorption of the H-I particles. The mean diameter of the H-I particles (0.148 μm) is identical with that (0.148 μm) obtained by TEM or found (0.148 μm) by the direct injection of the H-I particles into the channel using the carrier in which no adsorption occurs.

These data show that the adsorption of the H-I particles on the channel wall took place at the beginning of the column, thus making possible the use of the real value of V_0 for the calculation of d. Another important point to examine is whether the deposition of the particles of H-I is fully reversible because, if some particles are still deposited on the channell wall after the change of carrier solution, then the channel wall will gradually be fouled. A strong indication for the desorption of all of the material was the fact that no elution peak was obtained, even when the field strength was reduced to zero.

Haematite-II (H-II, $d^{TEM} = 0.248$ *μm).* Fig. 4 illustrates the variation of the retention ratio or of the calculated particle diameter for the H-II particles with the field strength at a constant flow-rate, and with the carrier flow-rate at a constant field strength. Using the optimum experimental conditions found (G = 9202 $cm\ s^{-2}$, $\dot{V}$ = 171 $cm^3\ h^{-1}$), the variation of the retention ratio or of the particle diameter for the H-II sample with the ionic strength of the carrier solution was investigated. Whereas at low ionic strengths the H-II–wall interactions are negligible, at higher electrolyte concentrations there is a limiting critical concentration (*ca.* $3 \cdot 10^{-2}$ M KNO_3) at

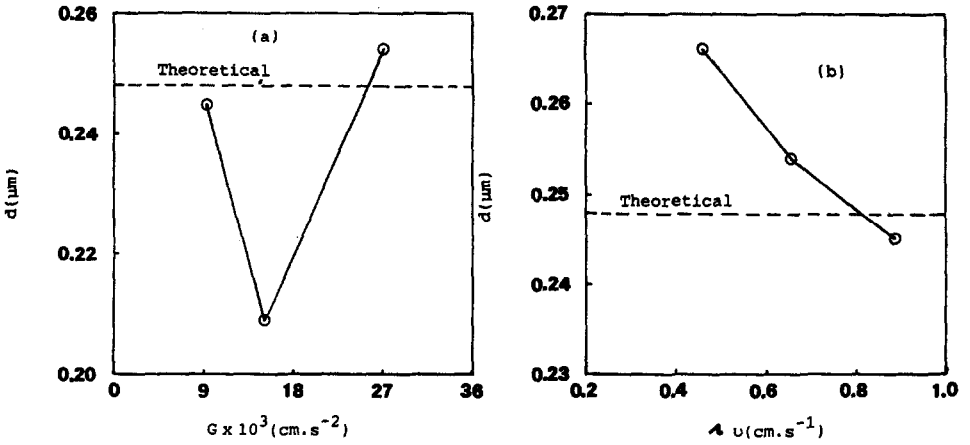

Fig. 4. Particle diameter for the haematite-II sample *versus* (a) field strength and (b) flow-rate. In both instances the SdFFF system II was used.

which adsorption of all of the H-II colloidal particles occurs at the beginning of the column. Variation of the carrier solution to one containing a lower electrolyte concentration (*ca.* 10^{-3} *M* KNO_3) released the total number of adherent H-II particles and gave a particle size (0.245 μm) in good agreement with that obtained by TEM (0.248 μm) or found (0.245 μm) when the colloidal particles were injected into the channel with the carrier solution in which no adsorption occurs.

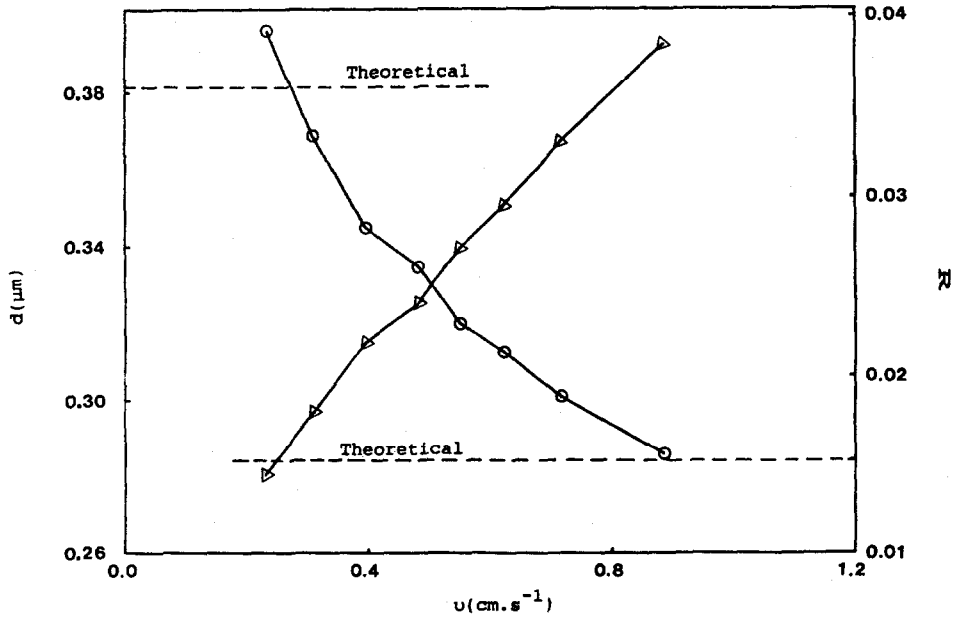

Fig. 5. Particle diameter (○) and retention ratio (△) *versus* carrier flow-rate for the TiO_2 colloidal sample in the SdFFF system II.

Interactions between titanium dioxide and the SdFFF channel wall

Fig. 5 shows the variation of the retention ratio and of the particle diameter for the TiO_2 particles with the carrier flow-rate at constant field strength (G = 9202 cm s^{-2}). Although the optimum flow-rate from Fig. 5 was found to be *ca.* 45 cm^3 h^{-1}, the investigation of the variation of the retention ratio or of the particle diameter for the TiO_2 sample with the ionic strength of the carrier solution was carried out at *ca.* 170 cm^3 h^{-1} in order to avoid long analysis times and broad peaks (Fig. 6).

The latter investigation showed that the critical electrolyte concentration for the total adsorption of the TiO_2 particles on the stainless-steel channel wall was that containing $3 \cdot 10^{-2}$ M KNO_3. Variation of the carrier solution to one containing a lower electrolyte concentration (*ca.* 10^{-3} M KNO_3) released all of the adherent TiO_2 particles and gave a particle size (0.302 μm) in good agreement with that (0.298 μm) obtained when the colloidal TiO_2 particles were injected into the channel with the carrier solution in which no adsorption occurs.

Fractionation of titanium dioxide and haematite-I by PBFFF

Fig. 7a shows the fractionation of the TiO_2 and H-I particles by the normal SdFFF procedure, which is based on the particle size difference, and Fig. 7b shows the fractionation of the same particles by the PBFFF technique, which is based on the total potential energy, V_{tot} (given by eqn. 16), difference. In the PBFFF technique the mixture was injected in the carrier solution containing $3 \cdot 10^{-2}$ M KNO_3. At this high electrolyte concentration all of the TiO_2 colloidal particles adhered at the beginning of the SdFFF stainless-steel channel wall, whereas all of the TiO_2 colloidal particles

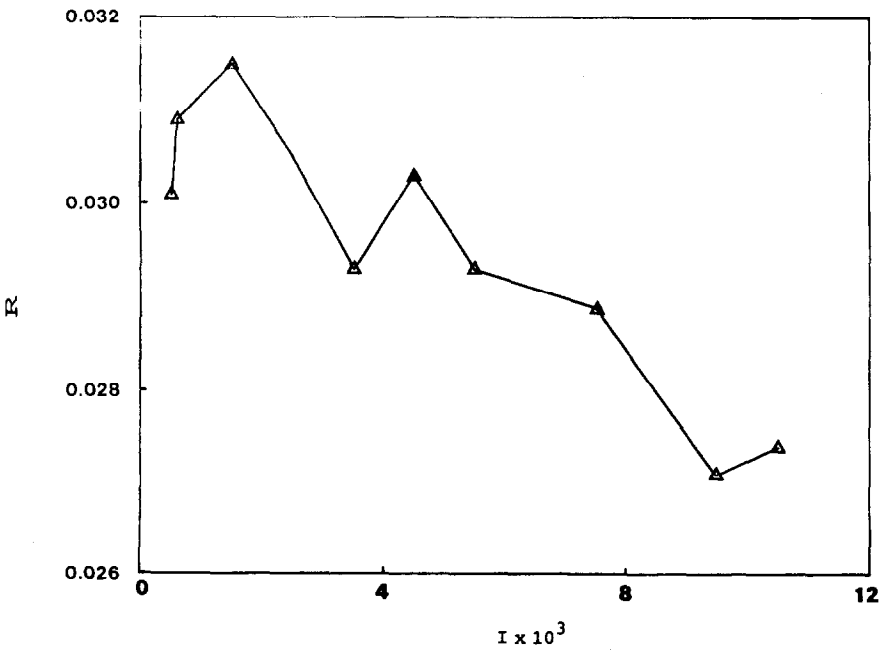

Fig. 6. Variation of the retention ratio for the TiO_2 sample with the ionic strength of the carrier solution. The SdFFF system II was used.

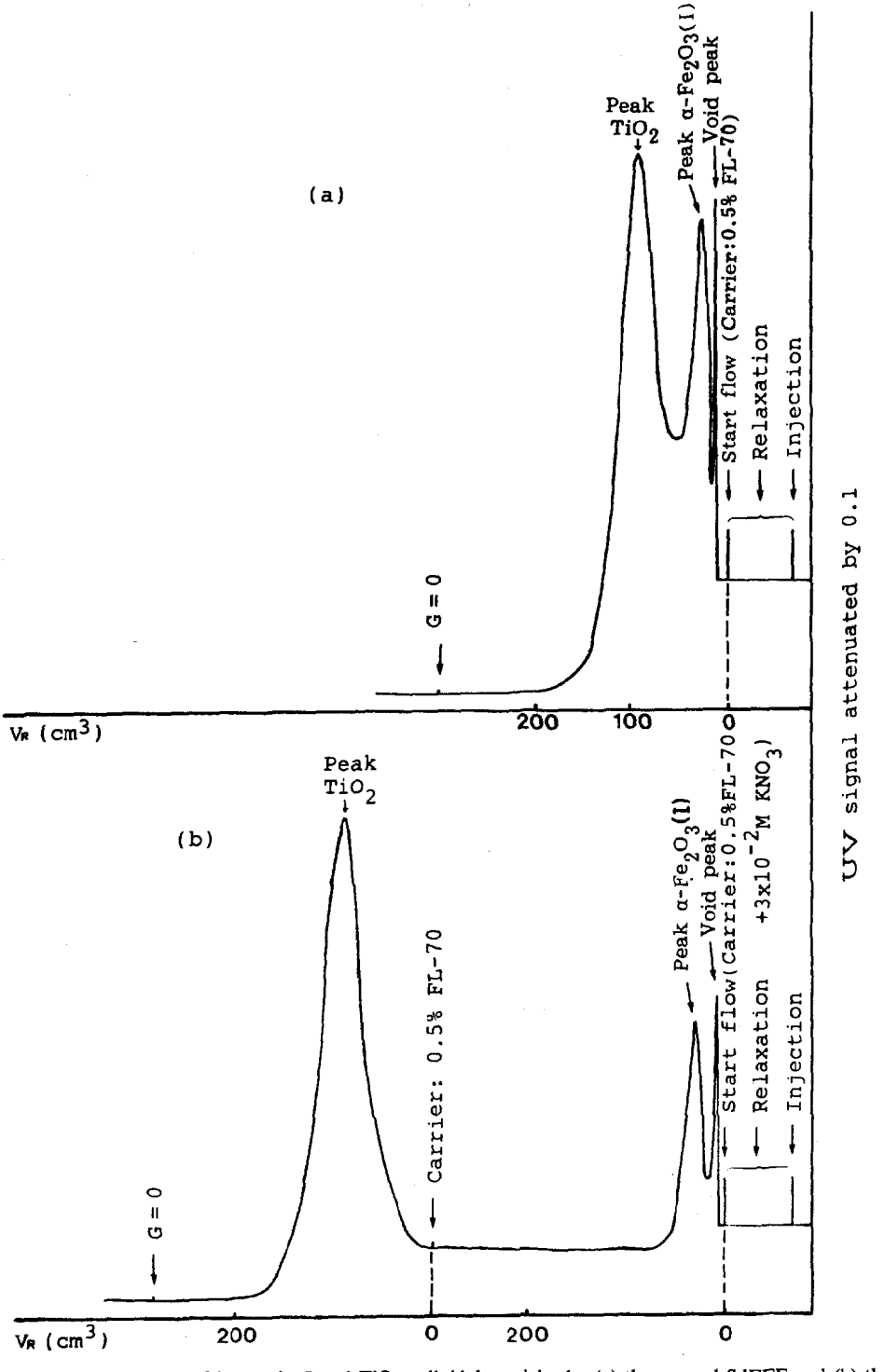

Fig. 7. Fractionation of haematite-I and TiO_2 colloidal particles by (a) the normal SdFFF and (b) the PBFFF technique.

adhered at the beginning of the H-I particles were eluted from the channel. The average diameter of the eluted H-I particles was found (by the PBFFF technique) to be 0.143 μm, in good agreement with that obtained by TEM (0.148 μm) or determined by normal SdFFF (0.150 μm) during the fractionation of TiO_2 and H-I particles. It must be pointed out that the particle diameter was obtained from eqn. 2 when the particles were run in the normal SdFFF mode, after the total adsorption following the PBFFF mode.

Changing the carrier solution to one containing only 0.5% detergent FL-70 released all of the adherent TiO_2 particles and gave a particle diameter (0.302 μm) in good agreement with that (0.298 μm) obtained during the fractionation of TiO_2 and H-I particles by the normal SdFFF technique.

The desorption of all of two colloids during the PBFFF procedure was verified by the fact that no elution peak was obtained even when the field strength was reduced to zero. A second indication for the desorption all of the material was the fact that the peaks of α-Fe_2O_3 and TiO_2 after adsorption and desorption of the particles (*cf.*, Fig. 7b) emerge without degradation, in contrast to the peaks in Fig. 7a. The different limiting electrolyte concentrations for the total adsorption of the TiO_2 and H-I colloidal particles on the SdFFF stainless-steel channel wall and hence the separation of the above particles by the PBFFF technique are due to the different total potential energies, V_{tot}, given by eqn. 16. Therefore, the separation of TiO_2 and H-I colloidal particles by the PBFFF technique is based on the particle size difference and/or on the Hamaker constant and the surface potential difference of the particles. The difference in diameters for the TiO_2 and H-I particles is known from the TEM pictures. Let us examine now whether or not the two samples have different Hamaker constants and surface potentials.

The Hamaker constant A_{132} ($= 1.02 \cdot 10^{-20}$ J) for the system steel–water–iron (III) oxide was calculated from eqn. 8, by taking $2.2 \cdot 10^{-19}$ J (A_{11}) for steel, which is the Hamaker constant for iron[15], $4.4 \cdot 10^{-20}$ J (A_{33}) for water, as calculated from the Lifshitz theory[11] (*cf.*, eqn. 9), and $6.2 \cdot 10^{-20}$ J (A_{22}) for haematite[15]. The Hamaker constant for haematite was also determined from eqn. 10 by surface tension measurements. This value ($7.0 \cdot 10^{-20}$ J), which was found to be equal to the value for TiO_2, appears to be much too high. As pointed out by Hogg *et al.*[12], it seems reasonable to assume that the Hamaker constant is approximately the same for inorganic oxides dispersed in an aqueous medium, as the surface are essentially similar, being composed primarily of oxygen anions. Thus, the Hamaker constant for the system steel–water–titanium dioxide approaches that for the system steel–water–iron (III) oxide and the separation of TiO_2 and H-I colloidal particles is not based on the Hamaker constant difference.

The surface potentials of haematite and TiO_2 were calculated from eqn. 12 by using for pH_{zpc} the values given by Hunter[16]: pH_{zpc}(α-Fe_2O_3) = 8.5 and pH_{zpc}(TiO_2, rutile) = 5.8. Therefore ψ(α-Fe_2O_3) = -15.6 mV and ψ(TiO_2) = -45.7 mV. The latter values show that the total potential energy, V_{tot}, at a given Hamaker constant, particle size and Debye–Hückel parameter, is less for the haematite sample than for TiO_2, contrary to our experimental results, according to which the heamatite sample is more stable than TiO_2 at an electrolyte concentration of $3 \cdot 10^{-2}$ *M* KNO_3. This is probably due to the fact that the value of pH_{zpc} used is referred to the rutile modification of TiO_2 and not to the anatase form. For this reason, the electrophoretic

mobilities of the TiO_2 and α-Fe_2O_3 particles were measured at various ionic strengths of the carrier solution.

From the latter, the ζ potentials were determined by using eqns. 13 and 14. At the critical electrolyte concentration $3 \cdot 10^{-2}$ M KNO_3, where the TiO_2 colloidal particles adhered to the SdFFF channel wall, whereas the α-Fe_2O_3 particles were

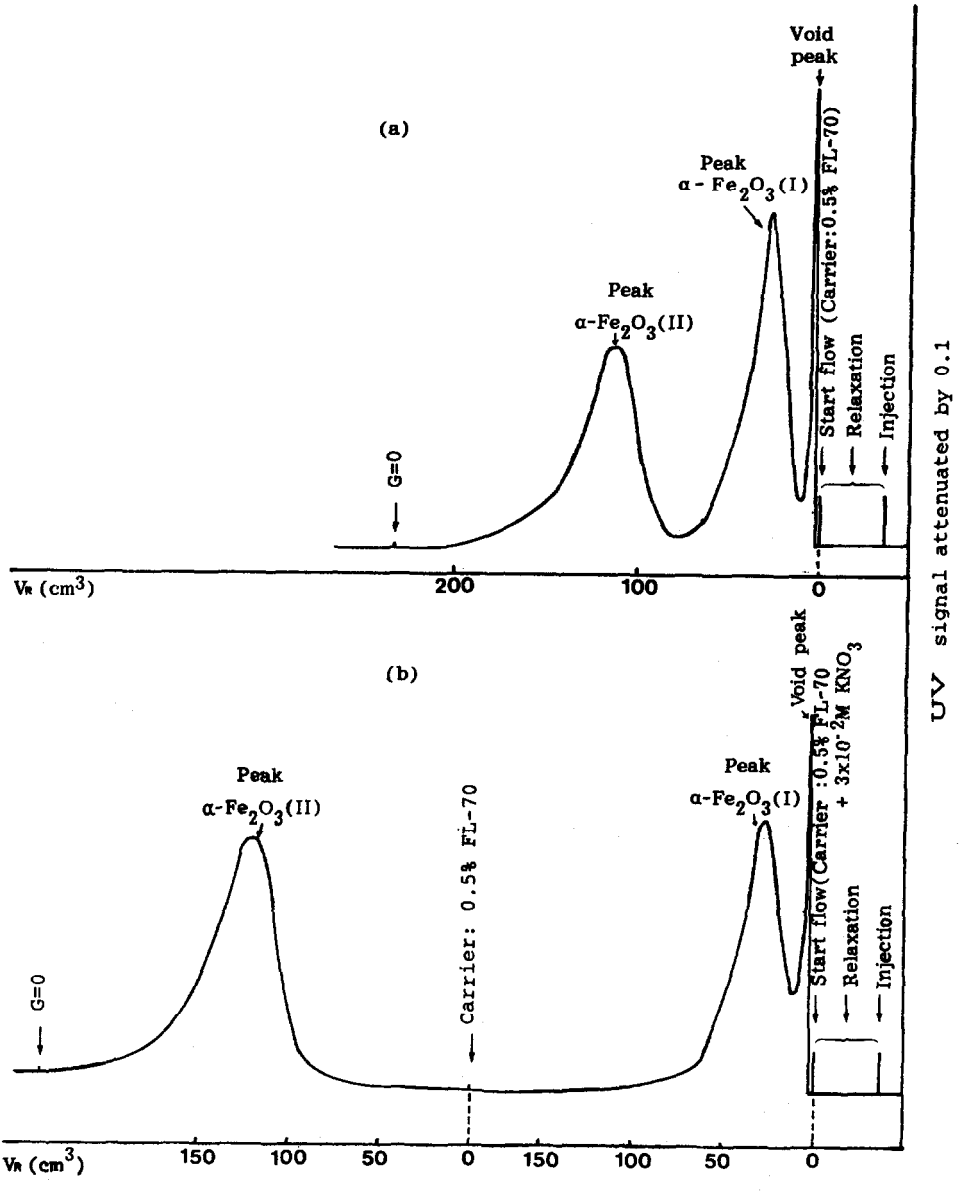

Fig. 8. Fractionation of haematite-I and haematite-II coloidal particles by (a) the normal SdFFF and (b) the PBFFF technique.

eluted from the channel, the ζ potentials were found to be $\zeta(\alpha\text{-}Fe_2O_3) = -20.4$ mV and $\zeta(TiO_2) = -19.1$ mV. These values are consistent with the experimental results showing that the fractionation of TiO_2 and H-I particles by the PBFFF technique is based on the particle size and the surface potential differences.

In the second example of fractionation by the PBFFF technique we used two samples of haematite with different particle diameters (Fig. 8). Here the separation is based only on the particle size difference, as the Hamaker constants and the surface potentials of the two samples are identical. Fig. 8a shows the fractionation of the haematite samples with different particle diameters by the normal SdFFF technique, and Fig. 8b that of the same samples by the PBFFF technique. The particle diameters obtained from eqn. 2 in the latter instance (0.151 μm for H-I and 0.244 μm for H-II) are in good agreement with those found by normal SdFFF (0.145 μm for H-I and 0.237 μm for H-II) or determined by TEM (0.148 μm for H-I and 0.248 μm for H-II).

ACKNOWLEDGEMENTS

We are grateful to Professor J. Calvin Giddings (University of Utah, U.S.A.), who supplied the SdFFF system, to Professor J. Lyklema (University of Wageningen, The Netherlands), who supplied the haematite samples, and to M. Barkoula for her kind assistance.

REFERENCES

1 H. Small, *J. Colloid Interface Sci.*, 48 (1974) 147.
2 V. K. F. Krebs and W. Wunderlich, *Angew. Makromol. Chem.*, 20 (1971) 203.
3 E. Ruckenstein, A. Marmur and W. N. Gill, *J. Colloid Interface Sci.*, 61 (1977) 183.
4 J. C. Giddings, F. J. F. Yang and M. N. Myers, *Anal. Chem.*, 46 (1974) 1917.
5 J. C. Giddings, G. Karaiskakis, K. D. Caldwell and M. N. Myers, *J. Colloid Interface Sci.*, 92 (1983) 66.
6 E. Dalas and G. Karaiskakis, *Colloids Surf.*, 28 (1987) 169.
7 G. Karaiskakis and E. Dalas, *J. Chromatogr. Sci.*, 26 (1988) 29.
8 A. Koliadima and G. Karaiskakis, *J. Liq. Chromatogr.*, 11 (1988) 2863.
9 G. Karaiskakis and A. Koliadima, *Chromatographia*, 28 (1989) 31.
10 M. E. Hansen and J. C. Giddings, *Anal. Chem.*, 61 (1989) 811.
11 J. N. Israelachvili, *Intermolecular and Surface Forces*, Academic Press, London, 1987, pp. 144–158.
12 R. Hogg, T. W. Healy and D. W. Fuerstenau, *Trans. Faraday Soc.*, 62 (1966) 1638.
13 P. C. Hiemenz, *Principles of Colloid and Surface Chemistry*, Marcel Dekker, New York, 1977, pp. 457–467.
14 E. Dalas, P. Koutsoukos and G. Karaiskakis, *Colloid. Polym. Sci.*, 268 (1990) 155.
15 R. J. Kuo and E. Matijevic, *J. Colloid Interface Sci.*, 78 (1980) 407.
16 R. J. Hunter, *Zeta Potential in Colloid Science*, Academic Press, London, 1981, p. 279.